Improved Signal Extraction from Fluorescence Immunoassay Image Sequences

Prasun Mahanti*, Thomas Taylor†, Douglas Cochran*, Mark Hayes‡ and Mathew Petkus‡
* Department of Electrical Engineering
Arizona State University
† Department of Mathematics and Statistics
Arizona State University
‡ Department of Chemistry and Biochemistry
Arizona State University

***Abstract*—A recently developed dynamic fluorescence immunoassay for the biomarker Myoglobin promises to provide detection of myocardial infarction within minutes. Signal extraction for this method is based on epifluorescence video microscopy, but is confounded by inhomogeneous spatial gain, intensity inhomogeneity or IIH. We present here a novel adaptive correction method which estimates the IIH from a video image sequence. This estimated IIH may be used to correct the image signal extraction process. The enhancement to detection limits and consistency of estimated concentrations are quantified, based on an improvement to SNR of approximately 9 dB.**

I. Introduction

Signal and image processing techniques have often aided clinical diagnostics. This work uses image processing methods to improve the extracted signal content from fluorescence immunoassay of Myoglobin. The experimental data is collected by an effective process of conglomerating tagged antigen Myoglobin [1] in rotating particle chains which promises to make the acquired time-varying fluorescent signal more distinguishable. Extending further from the signal estimation directly from the imaged fluorescence signal we find that there is an inherent defect associated with the imaging process making global thresholding ineffective. We propose an image distortion model to correct the defect. The correction involves estimation of the distortion in the first place from the true image and this is achieved by a novel surface fitting approach. The model is then used to correct an entire image sequence. Basic segmentation is then performed to extract the signal for different concentrations of the biochemical which ultimately gives us an estimation curve for the biochemical concentration with respect to the measured signal characteristics.

II. Fluorescence Immunoassay for biosensors

Immunoassays use immunological specificity for biochemical detection. The sensitivity of immunoassays is due to the unique selective binding properties of antibodies [2]. The signal is generated from another reagent used to label the antibody and the amount of signal is proportional to the number of binding events. In the immunometric design of immunoassay, there is an antibody coated solid phase and a labeled antibody which is specific for another part of the analyte molecule. The analyte is allowed to bind with the antibodies and a sandwich is formed with the target bound between the antibodies. When fluorescent labeling is done, it is called a fluorescence immunoassay.

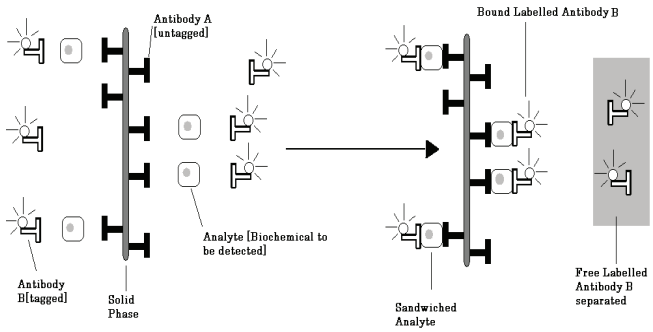

Fig. 1. Simulation Results

III. Data Extraction from Rotating Paramagnetic Chains

In a recently proposed technique, the distributed fluorescent signal spontaneously forms localized fluorescent signal objects [3]. The application of a magnetic field to a colloidal paramagnetic particle suspension causes them to build supraparticle chains. These chains are made to rotate in accordance to an rotating external magnetic field. The visible area of the rotating structures which correspond to the acquired image changes periodically and the surface bound fluorescent species contribute to the rotating signal objects.

This method of using rotating chains creates prominent intensity difference between signal objects and background in the captured image sequence by minimizing clutter and irrelevant intensity data.

IV. Problems in Image Data Analysis

Image segmentation is an obvious algorithmic approach to extracting signal from clutter and background. However, image segmentation algorithms employing global thresholding perform poorly due to the spatial intensity inhomogeneity (IIH) intrinsic to the image acquisition process. A globally selected threshold is found to be either too high or too

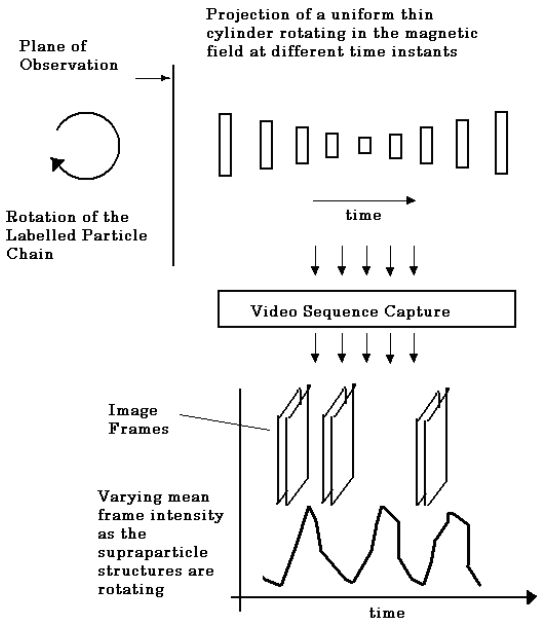

Fig. 2. Video sequence capture of rotating chain as a projection of the particle chain in the plane of image formation. The supra-particle chains have been compared to a rigid cylinder to show the change in projected area over time.

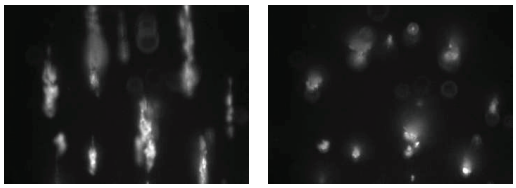

(a) parallel (b) perpendicular

Fig. 3. Images of rotating flulorescent chains at different orientations of the axis with respect to the imaging plane

low leading to an erroneous classification of foreground and background objects as can be seen in Fig. 4. The analysis of some frames where no labeled antibody has been added (control frames) shows the nature of the distortion without the presence of the signal. Removal of this distortion is an essential step before image segmentation and signal extraction.

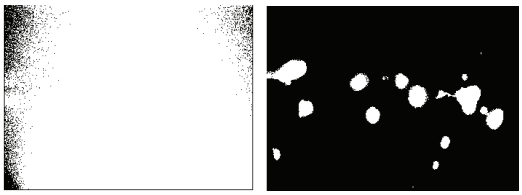

(a) Threshold too low (b) Threshold too high

Fig. 4. Effect of global thresholding in images

The distortion effects are introduced during image acquisition where different pixels of the image appear to be multiplied by different gains. The effect is caused by the intensity variation of light with distance as well as due to CCD sensor array imperfections [4] . In the literature, the effect has been studied under several names like vignetting, shading, uneven illumination, flat field and intensity inhomogeneity for example. The effective distortion can be modeled as a combination of additive and multiplicative parts. The image distortion of an image I_0 is thus modeled as

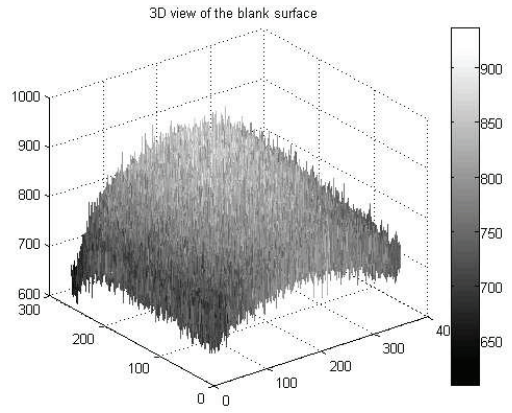

Fig. 5. Reconstruction of distortion surface

$$I = I_0 R_1 + R_2 \tag{1}$$

where R_1 is the multiplicative distortion and R_2 is the additive distortion.

V. ADAPTIVE IMAGE DISTORTION CORRECTION

Intensity inhomogeneity effects can be minimized by a proper set up of the imaging conditions [5], however in the current case, the light originating from the object is due to reflection as well as fluorescence. A source of illumination thus changes position spatially and temporally making it all the more necessary to determine the distortion effect dynamically. The image distortion model suggests the following distortion correction model. We choose to determine the multiplicative spatial component assuming the additive component to be small magnitude of uncorrelated noise.

$$I_0 = \frac{I - R_2}{R_1} \tag{2}$$

To estimate R_1 we use surface fitting among the well known methods [6] for shading correction. The control points for distortion surface fitting are selected dynamically. At the same time a binary matrix F is generated with 1's at pixels which can belong to a signal object. This is done by using a smoothed control frame to correct the distortion while accounting for not using the actual distortion surface. Our method of fitting the surface works by scanning each row or column of the control point matrix sequentially, fitting it to a quadratic function and stacking these fitted curves in order to get back the surface. The method involves the following steps:

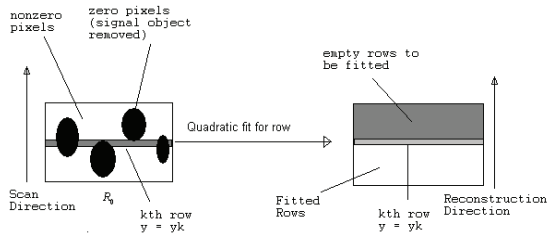

Fig. 6. Reconstruction of distortion surface

a) For each line from the control point matrix, a 2nd order fit is obtained in the least-square sense. Fitting rows and columns separately we get the two surfaces P and Q.

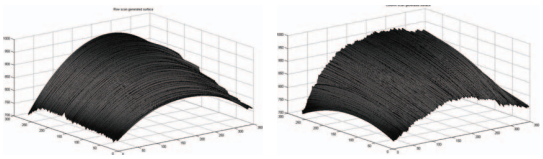

(a) Stacking of rows (P) (b) Stacking of columns (Q)

Fig. 7. Surfaces from stacking of quadratic curves

b) Writing the distortion surface as linear combination of the two surfaces with a parameter α, we get

$$R_{est} = \alpha P + (1 - \alpha)Q \tag{3}$$

The correct value of R_{est} would give a surface closest to the actual distortion surface R_1 and this surface would pass through the control point matrix such that the sum of squares of the difference between each pixel on R_{est} and the control point matrix is minimum.

c) We define the above said difference as the error E.

$$E = I \cap \overline{F} - R_{est} \cap \overline{F} \tag{4}$$

where I is the image frame and R_{est} is the estimated distortion. Hence we can formulate the square-error minimization problem

$$\alpha = \arg\min_{\alpha} \{ \sum_{x} \sum_{y} (E)^2 \} \tag{5}$$

The summation is over both directions x and y of the region of support. Minimizing the error we get

$$\alpha = \frac{\sum_{x} \sum_{y} (Q \cap \overline{F} - I \cap \overline{F})}{\sum_{x} \sum_{y} (Q \cap \overline{F} - P \cap \overline{F})} \tag{6}$$

This value of α is used in 3 to get the distortion surface. The estimated distortion surface is then used to divide the image and then the leveled signal regions are extracted by standard image segmentation.

VI. ESTIMATION OF CONCENTRATION FROM IMAGE SEQUENCES.

From each image frame we get multiple signal regions as can be seen below. The sum of the intensity values from the signal regions are used to quantify the intensity of the frame.

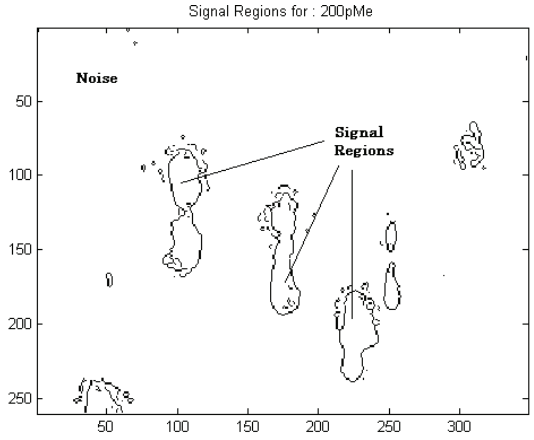

Fig. 8. Signal regions from image

Since the signal objects rotate, they vary in size periodically giving rise to a temporal signal which represents the image sequence.

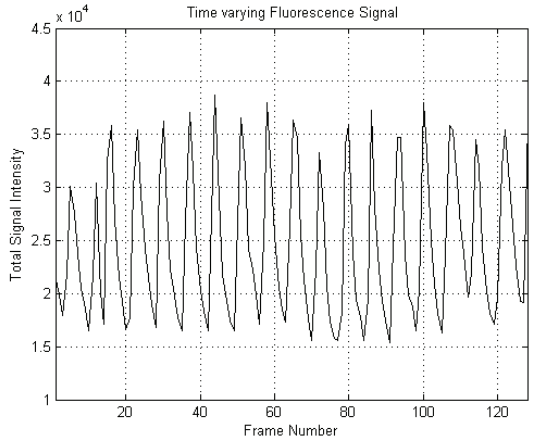

Fig. 9. Time-varying fluorescence signal

Each data point in the signal corresponds to the total signal intensity of an image frame and the average signal energy serves in turn relates to the Myoglobin concentration. The average signal energy is defined as

$$E_{S,avg} = \frac{1}{T} \sum_{n} [x(n)]^2 \tag{7}$$

where $x(n)$ is the sum of intensities of all the signal regions of the nth frame and T is the total number of frames. It is also found that the noise is spatially stationary which allows us to define the noise energy as

$$E_{N,frame} = N_s(n)\sigma(n)^2 \tag{8}$$

where $N_s(n)$ is the number of signal pixels for the nth frame and $\sigma(n)^2$ is the variance of the non-signal regions for the nth frame. Thus, the SNR in dB is given by

$$SNR_{dB} = 10\log_{10}\left(\frac{\sum_{n=1}^{T}[x(n)]^2}{\sum_{n=1}^{T}N_s(n)\sigma(n)^2}\right) \quad (9)$$

The application of our algorithm to multiple experiments, including three at each of eight distinct concentrations, gives us the following concentration-intensity curve. In most cases the points fall over one another indicating a probable low variance across different observations.

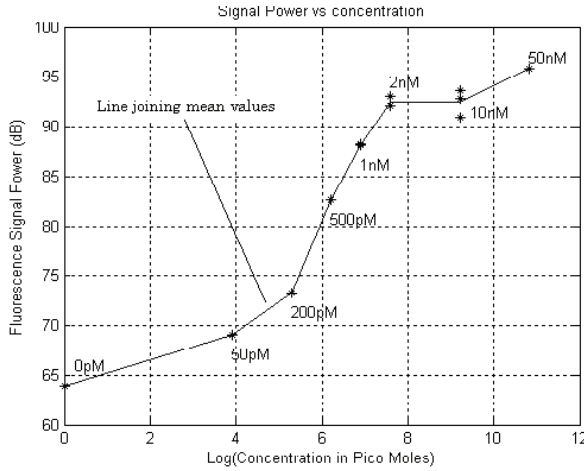

Fig. 10. Signal power for varying concentrations of biochemical

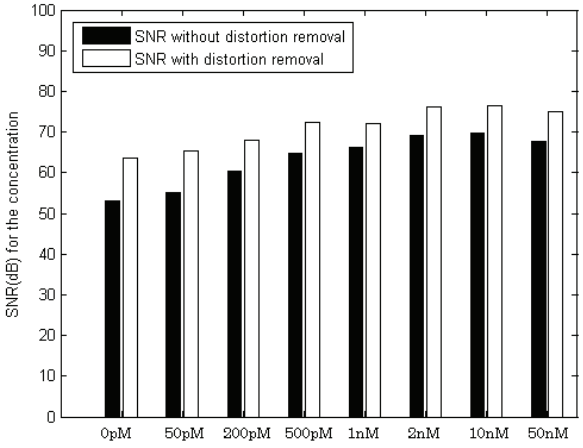

Fig. 11. SNR with and without distortion removal

Also, a higher SNR is always seen for the case where the distortion was removed which is as expected as the noise power is far higher if the distortion is not removed. Approximately, a 9dB difference over the entire range of concentration is observed.

VII. CONCLUSION

We have initiated and explored the possibilities of a novel biochemical concentration estimator using signal processing techniques on digital video data of rotating magnetic bead fluorescence immunoassay. We have shown that with estimation and elimination of image distortion artifacts due to nonlinearities in the optical image acquisition process, we can improve signal extraction by a large margin. The concentration estimator curve we obtain shows high levels of sensitivity and successfully correlates with theoretical principles of analytical chemistry. The rapid automatic concentration estimation technology promised by these results can be incorporated in diagnostic medical devices for timely guidance of medical intervention in a number of high consequence situations, including the motivating example of potential acute myocardial infarction.

REFERENCES

[1] M. Petkus, A.A. Garcia, M.A. Hayes, T. Taylor, and P. Mahanti, "Competitive Modulated Immunoassays for Serum Myoglobin," *The Analyst*, vol. 134, 2009.

[2] D. Wild et al., *The immunoassay handbook*, Elsevier Amsterdam:, 2005.

[3] A.K. Vuppu, A.A. Garcia, M.A. Hayes, K. Booksh, P.E. Phelan, R. Calhoun, and S.K. Saha, "Phase sensitive enhancement for biochemical detection using rotating paramagnetic particle chains," *Journal of Applied Physics*, vol. 96, pp. 6831, 2004.

[4] Diagonistic Instruments, "Correction of ccd image imperfections," World Wide Web electronic publication, 2004.

[5] J.C. Russ, *The Image Processing Handbook*, CRC Press, 2006.

[6] T. Dejan, L. Bostjan, and P. Franjo, "A Comparison of Retrospective Shading Correction Techniques," in *International Conference on Pattern Recognition (ICPR00)*, 2000, vol. 3, pp. 564–567.